

Study of $\psi(2S)$ decays into $\gamma K^+ K^-$ and $\gamma \pi^+ \pi^-$

M. Ablikim,¹ J. Z. Bai,¹ Y. Ban,² X. Cai,¹ H.F. Chen,³ H.S. Chen,¹ H.X. Chen,¹ J.C. Chen,¹ Jin Chen,¹ Y.B. Chen,¹ Y.P. Chu,¹ Y.S. Dai,⁴ L.Y. Diao,⁵ Z.Y. Deng,¹ Q.F. Dong,⁶ S.X. Du,¹ J. Fang,¹ S.S. Fang,^{1,*} C.D. Fu,⁶ C.S. Gao,¹ Y.N. Gao,⁶ S.D. Gu,¹ Y.T. Gu,⁷ Y.N. Guo,¹ Z.J. Guo,^{8,†} F.A. Harris,⁸ K.L. He,¹ M. He,⁹ Y.K. Heng,¹ J. Hou,¹⁰ H.M. Hu,¹ J.H. Hu,¹¹ T. Hu,¹ X.T. Huang,⁹ X.B. Ji,¹ X.S. Jiang,¹ X.Y. Jiang,¹² J.B. Jiao,⁹ D.P. Jin,¹ S. Jin,¹ Y.F. Lai,¹ G. Li,^{1,‡} H.B. Li,¹ J. Li,¹ R.Y. Li,¹ S.M. Li,¹ W.D. Li,¹ W.G. Li,¹ X.L. Li,¹ X.N. Li,¹ X.Q. Li,¹⁰ Y.F. Liang,¹³ H.B. Liao,¹ B.J. Liu,¹ C.X. Liu,¹ F. Liu,¹⁴ Fang Liu,¹ H.H. Liu,¹ H.M. Liu,¹ J. Liu,² J.B. Liu,¹ J. P. Liu,¹⁵ Jian Liu,⁸ Q. Liu,⁸ R.G. Liu,¹ Z.A. Liu,¹ Y.C. Lou,¹² F. Lu,¹ G.R. Lu,¹² J.G. Lu,¹ A. Lundborg,¹⁶ C.L. Luo,¹⁷ F.C. Ma,⁵ H.L. Ma,¹⁸ L.L. Ma,^{1,§} Q.M. Ma,¹ Z.P. Mao,¹ X.H. Mo,¹ J. Nie,¹ S.L. Olsen,⁸ R.G. Ping,¹ N.D. Qi,¹ H. Qin,¹ J.F. Qiu,¹ Z.Y. Ren,¹ G. Rong,¹ X.D. Ruan,⁷ L.Y. Shan,⁸ L. Shang,⁸ C.P. Shen,⁸ D.L. Shen,¹ X.Y. Shen,¹ H.Y. Sheng,¹ H.S. Sun,¹ S.S. Sun,¹ Y.Z. Sun,¹ Z.J. Sun,¹ X. Tang,¹ G.L. Tong,¹ G.S. Varner,⁸ D.Y. Wang,^{1,¶} L. Wang,¹ L.L. Wang,¹ L.S. Wang,¹ M. Wang,¹ P. Wang,¹ P.L. Wang,¹ Y.F. Wang,¹ Z. Wang,¹ Z.Y. Wang,¹ Zheng Wang,¹ C.L. Wei,¹ D.H. Wei,¹ Y. Weng,¹ U. Wiedner,¹⁹ N. Wu,¹ X.M. Xia,¹ X.X. Xie,¹ G.F. Xu,¹ X.P. Xu,¹⁴ Y. Xu,¹⁰ M.L. Yan,³ H.X. Yang,¹ Y.X. Yang,¹¹ M.H. Ye,¹⁸ Y.X. Ye,³ G.W. Yu,¹ C.Z. Yuan,¹ Y. Yuan,¹ S.L. Zhang,¹ Y. Zeng,²⁰ B.X. Zhang,¹ B.Y. Zhang,¹ C.C. Zhang,¹ D.H. Zhang,¹ H.Q. Zhang,¹ H.Y. Zhang,¹ J.W. Zhang,¹ J.Y. Zhang,¹ S.H. Zhang,¹ X.Y. Zhang,²¹ Yiyun Zhang,¹³ Z.X. Zhang,² Z.P. Zhang,³ D.X. Zhao,¹ J.W. Zhao,¹ M.G. Zhao,¹ P.P. Zhao,¹ W.R. Zhao,¹ Z.G. Zhao,^{1,**} H.Q. Zheng,² J.P. Zheng,¹ Z.P. Zheng,¹ L. Zhou,¹ K.J. Zhu,¹ Q.M. Zhu,¹ Y.C. Zhu,¹ Y.S. Zhu,¹ Z.A. Zhu,¹ B.A. Zhuang,¹ X.A. Zhuang,¹ and B.S. Zou¹

(BES Collaboration)

¹*Institute of High Energy Physics, Beijing 100049, People's Republic of China*

²*Peking University, Beijing 100871, People's Republic of China*

³*University of Science and Technology of China, Hefei 230026, People's Republic of China*

⁴*Zhejiang University, Hangzhou 310028, People's Republic of China*

⁵*Liaoning University, Shenyang 110036, People's Republic of China*

⁶*Tsinghua University, Beijing 100084, People's Republic of China*

⁷*Guangxi University, Guilin 541004, People's Republic of China*

⁸*University of Hawaii, Honolulu, HI 96822, USA*

⁹*Shandong University, Jinan 250100, People's Republic of China*

¹⁰*Nankai University, Tianjin 300071, People's Republic of China*

¹¹*Guangxi Normal University, Guilin 541004, People's Republic of China*

¹²*Henan Normal University, Xinxiang 453002, People's Republic of China*

¹³*Sichuan University, Chengdu 610064, People's Republic of China*

¹⁴*Huazhong Normal University, Wuhan 430079, People's Republic of China*

¹⁵*Wuhan University, Wuhan 430072, People's Republic of China*

¹⁶*Uppsala University, SE-75121 Uppsala, Sweden*

¹⁷*Nanjing Normal University, Nanjing 210097, People's Republic of China*

¹⁸*China Center for Advanced Science and Technology (CCAST)*

¹⁹*Bochum University, D-44780 Bochum, Germany*

²⁰*Hunan University, Changsha 410082, People's Republic of China*

²¹*Shandong University, Jinan 250100, People's Republic of China*

(Dated: October 29, 2018)

Radiative charmonium decays from the BESII sample of 14×10^6 $\psi(2S)$ -events into two different final states, $\gamma K^+ K^-$ and $\gamma \pi^+ \pi^-$, are analyzed. Product branching fractions for $\psi(2S) \rightarrow \gamma X \rightarrow \gamma \pi^+ \pi^-$, $\gamma K^+ K^-$ are given, where $X = f_2(1270)$, $f_0(1500)$, and $f_0(1710)$ in $\pi^+ \pi^-$ and $f_2(1270)$, $f_2'(1525)$, and $f_0(1700)$ in $K^+ K^-$. An angular analysis gives the ratios of the helicity projections for the $f_2(1270)$ in $\psi(2S) \rightarrow \gamma f_2(1270) \rightarrow \gamma \pi^+ \pi^-$.

PACS numbers: 13.20.Ce, 13.20.Gd, 13.28.-b

*Current address: DESY, D-22607, Hamburg, Germany

†Current address: John Hopkins University, Baltimore, MD 21218, USA

‡Current address: Université Paris XI, LAL, 91898 ORSAY Cedex, France

§Current address: University of Toronto, Toronto M5S 1A7, Canada

¶Current address: CERN, CH-1211 Geneva 23, Switzerland

**Current address: University of Michigan, Ann Arbor, MI 48109, USA

I. INTRODUCTION

Several exotic QCD states, such as glueballs, hybrids or multiquarks, are expected to have masses between 1 and 2.5 GeV/ c^2 [1]. Radiative J/ψ and $\psi(2S)$ decays are traditionally regarded as gluon-rich environments; such decays, although well investigated, are still promising for the discovery and identification of QCD exotica. For example, in radiative decays into pseudoscalars, two of the most promising glueball candidates, the $f_0(1500)$ and the $f_0(1710)$, are seen [1]. Several high precision partial wave analyses of radiative J/ψ decays have been performed [2], and a recent BES-paper presented an analysis of a high statistics sample of $\psi(2S)$ decays, without a partial wave analysis [3]. This paper updates the $\psi(2S)$ radiative decays [3, 4] with $\gamma K^+ K^-$ and $\gamma \pi^+ \pi^-$ final states, giving access to scalar and tensor intermediate states.

Within the quark model [5], the $\psi(2S)$ is believed to have 2^3S_1 as its main component, and the J/ψ is the 1^3S_1 $c\bar{c}$ -state. This gives a $\psi(2S)$ with a behavior that differs from J/ψ only due to the difference in energy scale and in the radial wave function. The so-called 12%-rule from perturbative QCD (pQCD) relates the branching fractions of the two states into a particular hadronic final state (*h.f.s.*):

$$\begin{aligned} \frac{BR(\psi(2S) \rightarrow h.f.s.)}{BR(J/\psi \rightarrow h.f.s.)} &\stackrel{pQCD}{=} \frac{BR(\psi(2S) \rightarrow ggg)}{BR(J/\psi \rightarrow ggg)} \quad (1) \\ &\simeq \frac{BR(\psi(2S) \rightarrow e^+e^-)}{BR(J/\psi \rightarrow e^+e^-)} \\ &= \frac{(7.43 \pm 0.06) \times 10^{-3}}{(5.94 \pm 0.06) \times 10^{-2}} \\ &\simeq 12.5\%, \end{aligned}$$

where the branching fractions are from Ref. [1]. A radiative decay mode would be similar, but would proceed via one photon and two gluons, exchanging one power of α_s with α in the coupling [6, 7, 8, 9, 10]. A large violation of the 12%-rule was first observed in 1983 in $\psi(2S)$ decays to $\rho\pi$ and $K^{*+}K^- + c.c.$ by MARKII; it became known as the $\rho\pi$ -puzzle [11]. Since then, many two-body decay modes have been compared, of which some obey and some violate the rule [1, 12].

The analysis uses the BESII data sample of $(14 \pm 0.56) \times 10^6$ $\psi(2S)$ -events [13], corresponding to an integrated luminosity of (19.72 ± 0.86) pb $^{-1}$ [14], and a set of continuum data at $\sqrt{s} = 3.65$ GeV, (6.42 ± 0.24) pb $^{-1}$ [15], also measured with the BESII detector.

II. THE BESII DETECTOR

BESII is a cylindrical multi-component detector, described in detail in Refs. [16] and [17]. Around the beam-pipe is a 12-layer straw vertex chamber, which provides trigger and track information. Located radially outside, there is a 40-layer open-cell geometry main

drift chamber (MDC), covering 85% of the solid angle. The MDC is used for tracking and particle identification using dE/dx -techniques. The momentum resolution is $\sigma_p/p = 1.78\% \sqrt{1+p^2}$ [GeV/ c], and the MDC $(dE/dx)/E$ resolution for hadron tracks is $\sim 8\%$. Particle identification by energy loss techniques is complemented by a measurement of the time-of-flight (TOF) from the interaction point to 48 scintillation counters surrounding the MDC (time resolution ~ 200 ps for hadrons). Outside the TOF-scintillators is a 12 radiation length lead-gas barrel shower counter (BSC), which measures the energy of electrons and photons over $\sim 80\%$ of the total solid angle with a resolution of $\sigma_E/E = 22\%/\sqrt{E}$ [GeV]. In addition, the iron flux return, outside the solenoid coil (0.4 T axial field), is instrumented with three double layers of counters for identification of muons with momenta larger than 0.5 GeV/ c . The cylindrical structure is closed by end-caps.

III. EVENT SELECTION

Events with at least one photon and two oppositely charged tracks with good helix fits and complete covariance matrices are selected. End-cap information is used to reject background with extra charged particles in the end-cap region, but only events within the well-understood barrel detectors are included in the analysis. The polar angles of the charged particles are required to fulfill $|\cos\theta_{\pm}| < 0.8$ for K^+K^- and $|\cos\theta_{\pm}| < 0.65$ for $\pi^+\pi^-$, where θ_{\pm} is the angle of the charged particle with respect to the beam axis. The vertex of the two charged tracks is required to satisfy $V_{xy} = \sqrt{V_x^2 + V_y^2} < 1.5$ cm and $|V_z| < 15$ cm, where V_x , V_y , and V_z are the x , y , and z coordinates of the point of closest approach of each charged track to the beam axis. The photon with the highest energy is tested for quality: it must be within the barrel detector, it must have its first hit in the BSC inside the first 12 layers out of 24, it must be separated from charged tracks by at least 15° in the xy-plane at the entrance of the BSC, and the photon direction from the origin to the BSC must agree within 35° with the shower direction in the BSC.

A. Particle identification

The most abundant e^+e^- reactions at GeV-energies are QED processes, mainly $e^+e^- \rightarrow e^+e^-$ and $e^+e^- \rightarrow \mu^+\mu^-$. In cases where there is initial or final state radiation, the event could be misidentified as $\gamma\pi^+\pi^-$ or γK^+K^- . Muons are rejected using muon chamber information; this is especially important in the $\gamma\pi^+\pi^-$ channel, therefore the stricter angular cut. Bhabha events, $e^+e^- \rightarrow \gamma e^+e^-$, are rejected using the dE/dx χ -value under the e^\pm hypothesis ($\chi_e = (dE/dx_{measured} - dE/dx_{expected\ for\ e^\pm})/\sigma_{dE/dx\ e^\pm}$) combined with the en-

ergy deposited in the calorimeter E_{cal} and the momentum p_{MDC} . To reject background from $e^+e^- \rightarrow (\gamma)e^+e^-$, the selected sample is required to satisfy

$$\chi_+^2 + \chi_-^2 + 6 \left(\sqrt{\left(\frac{E_{cal.}}{p_{MDC}}\right)_+^2 + \left(\frac{E_{cal.}}{p_{MDC}}\right)_-^2} - 2 \right)^2 > 5^2. \quad (2)$$

The TOF and dE/dx measurements of the two charged tracks and a kinematic fit with four degrees of freedom are used to calculate χ^2 -values for the overall event-hypothesis: $\gamma\pi^+\pi^-$ or γK^+K^- . A confidence level of better than 1% is required for each event sample, and for ambiguous cases, the most likely assignment is chosen. After all requirements, the overall detection and event selection efficiency is $\sim 15\%$ (see Table I and II for exact numbers). The probability that a γK^+K^- event is selected as a $\gamma\pi^+\pi^-$ event is 0.17%, and the probability that a $\gamma\pi^+\pi^-$ event is selected as a γK^+K^- event is 0.14%, from Monte Carlo simulation.

B. Background

A carefully checked Geant3-based Monte Carlo program [18] is used to determine invariant mass resolution ($< 10 \text{ MeV}/c^2$ for $m_{\pi^+\pi^-}$ and for $m_{K^+K^-}$), angular efficiency, absolute efficiency, and background suppression. Using this program, the contributions from QED-processes after event selection are found to be small (dominated by $15 \pm 2 \gamma\mu^+\mu^-$ events in $\gamma\pi^+\pi^-$). However, both QED backgrounds and non-resonant hadronic signals are estimated using the continuum data sample, where the main contributor to the non-resonant background is found to be initial-state-radiation and subsequent ρ or ϕ -formation. This was checked for the ρ , and measurement agreed with calculations using a structure function approach [2, 19]. The full continuum contribution is assumed to be incoherent with the signal. Resonant background sources are checked individually using known cross sections and simulation to determine the acceptance of the selection criteria [1, 20, 21]. The main resonant background to both channels is found to be $\psi(2S) \rightarrow \pi^0\pi^+\pi^-$, which has been measured with great precision by BESII [12] using partial wave analysis. A Monte Carlo generated sample with the same angular and energy distribution as found in Ref. [12] is used, and 72 ± 5 misidentified background events in $\gamma\pi^+\pi^-$ and 4.9 ± 0.5 misidentified events in γK^+K^- are obtained. The signal and the background estimates are shown in Figs. 1 and 2.

IV. INTERMEDIATE RESONANCES

From spin-parity conservation, any intermediate resonance X in $e^+e^- \rightarrow \psi(2S) \rightarrow \gamma X \rightarrow \gamma K^+K^-$, $\gamma\pi^+\pi^-$ must have $J^{PC} = 0^{++}$, 2^{++} , or higher even spins. To

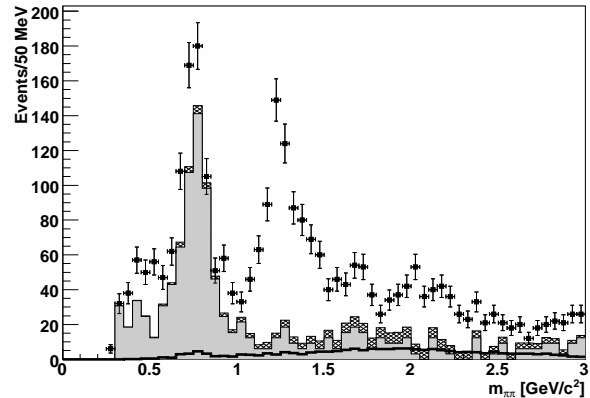


FIG. 1: The $m_{\pi^+\pi^-}$ distribution for $\psi(2S) \rightarrow \gamma\pi^+\pi^-$ candidate events (dots with error bars), along with the estimated background. The thick line corresponds to the background from $\psi(2S) \rightarrow \pi^0\pi^-\pi^+$ using the branching fraction from [1], the filled histogram corresponds to the continuum data, and the hatched histogram to a background estimate including the continuum and misidentified $\psi(2S) \rightarrow \pi^0\pi^-\pi^+$ -events. All contributions are scaled to correspond to the integrated luminosity of the $\psi(2S)$ data set. The histogram is not acceptance corrected.

investigate the resonance structure, the invariant mass spectra of the two pseudoscalar systems are fitted.

A. Previous observations

A partial wave analysis of BESII $J/\psi \rightarrow \gamma\pi\pi$ -data [22] required an $f_2(1270)$ at $m = 1262_{-2}^{+1} \pm 6 \text{ MeV}/c^2$, a 0^{++} -state at $1466 \pm 6 \pm 16 \text{ MeV}/c^2$, and a 0^{++} -state at $1.7 \text{ GeV}/c^2$ to fit the data properly. Due to the large $\rho\pi$ -background in J/ψ decays, the focus was on structures below $2 \text{ GeV}/c^2$, but it is worth mentioning that a peak around $2.1 \text{ GeV}/c^2$ was observed; this was the case also in γK^+K^- . In γK^+K^- , the $f_2'(1525)$ and $f_0(1710)$ were prominent [23].

An earlier analysis, using a smaller sample of $(3.90 \pm 0.21) \times 10^6$ good quality $\psi(2S)$ -events from BESII and using a $\tau^+\tau^-$ background sample at $\sqrt{s} = 3.55 - 3.6 \text{ GeV}$, showed a clear $f_2(1270)$ [$BR(\psi(2S) \rightarrow \gamma f_2(1270)) = (2.12 \pm 0.19 \pm 0.32) \times 10^{-4}$], an $f_0(1710)$ signal in $\gamma\pi\pi$ [$BR(\psi(2S) \rightarrow \gamma f_0(1710)) \times BR(f_0(1710) \rightarrow \pi\pi) = (3.01 \pm 0.41 \pm 1.24) \times 10^{-5}$], and a clear $f_0(1710)$ [$BR(\psi(2S) \rightarrow \gamma f_0(1710)) \times BR(f_0(1710) \rightarrow K^+K^-) = (3.02 \pm 0.45 \pm 0.66) \times 10^{-5}$], and a less clear $f_2'(1525)$ in γK^+K^- [4].

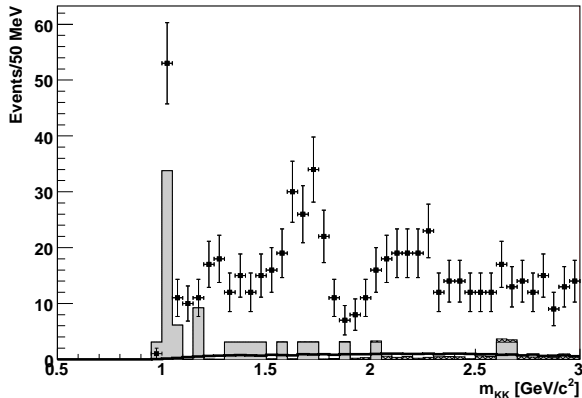


FIG. 2: The $m_{K^+K^-}$ distribution in $\psi(2S) \rightarrow \gamma K^+ K^-$ candidate events (dots with error bars) along with the estimated background. The thick line corresponds to the maximum background from $\psi(2S) \rightarrow K^+ K^- \pi^0$, which could be important if it is close to its upper limit [1]. The filled histogram corresponds to the scaled continuum, and the hatched histogram to a background estimate including the continuum and misidentified $\psi(2S) \rightarrow \pi^0 \pi^+ \pi^-$ -events. All contributions are scaled to correspond to the integrated luminosity of the $\psi(2S)$ data set. The histogram is not acceptance corrected.

B. Fit shape

The 0^{++} resonances are modeled as constant width Breit Wigner functions, with $1 + \cos^2 \theta_\gamma$ angular distributions. The 2^{++} resonances are modeled as Blatt Weisskopf damped d-wave shapes (with parameters as in Ref. [24] and angular distributions according to Eq. (4)). Masses and widths are taken from the Particle Data Group Compilation [1]. For simplicity any possible nonresonant production and background component is assumed to follow three-body phase space. All resonances are treated as incoherent. The unbinned meson-meson invariant mass spectrum is fitted with a log likelihood method, and the scaled background component from the continuum data sample and the simulated $\psi(2S) \rightarrow \pi^0 \pi^+ \pi^-$ background are included in the fit but with the opposite sign.

C. Fit quality

The quality of different log likelihood fits to the same data set can be compared since the ratio

$$R = -2 \ln \left| \frac{\mathcal{L}(fit_A)}{\mathcal{L}(fit_B)} \right| \quad (3)$$

follows a χ^2 -distribution [25]. The number of degrees of freedom for this χ^2 -distribution is given by the number of free parameters in fit_B minus the number of free parameters in fit_A . In this way, the difference in log likelihood

is used for an hypothesis test, for instance to determine the necessity of weakly needed resonances such as the $f_0(1500)$ in $\gamma \pi^+ \pi^-$ and the $f'_2(1525)$ in $\gamma K^+ K^-$. Another measure of the quality of the overall fit is obtained using a Pearson's χ^2 -test.

V. RESONANCES IN $\gamma \pi^+ \pi^-$

The fit to the two-pion invariant mass spectrum between 1 and 3 GeV/c^2 allows the determination of the number of events and the product decay branching fractions of $\psi(2S) \rightarrow \gamma X \rightarrow \gamma \pi^+ \pi^-$ where $X = f_2(1270)$, $f_0(1500)$, $f_0(1710)$, or a high mass component modeled here with $f_4(2050)$ and $f_0(2200)$ (Table I). The full fit, binned as in Fig. 3, has a Pearson's χ^2/DOF of 45.7/39. Note that the invariant mass peak near the $f_2(1270)$ is lower in this data set than the central value given by the Particle Data Group [1] (Fig. 3), and the branching fraction into $f_2(1270)$ is almost twice as large as in the corresponding BES I measurement [4]. The branching fraction into $f_0(1710)$ agrees with the BES I measurement, and for $f_0(1500)$ a branching fraction was not given by BES I. We use the χ^2 -hypothesis test (Section IV C) to check whether the inclusion of the $f_0(1500)$ improves the fit enough to motivate the one extra fit parameter. Removing the $f_0(1500)$ here changed the log likelihood such that $R = 6.2$ (Eq. 3). In a χ^2 -distribution with one degree of freedom, the probability to be above 6.2 is 1.28%, and, since $1.28\% < 5\%$, the $f_0(1500)$ is accepted at the 5% level. The high mass region, which is fitted with $f_4(2050)$ and $f_0(2200)$, can also be well fitted by alternative combinations of resonances; combinations with $f_2(1810)$, $f_0(2020)$, $f_2(2150)$, $f_4(2050)$, $f_0(2200)$, and a free mass and free width state have been tested. The selected fit is the best, but since other alternatives are not ruled out they are used to estimate the systematic uncertainty to the other branching fractions. In one version of the fit, the event excess in the region between two-pion threshold and 800 MeV/c^2 (Fig. 1) is fitted with an additional σ -shape. This is used to give a measure of the

TABLE I: Number of selected events and product branching fractions in the $\psi(2S) \rightarrow \gamma X \rightarrow \gamma \pi^+ \pi^-$ channel. The efficiency at the central resonance mass is determined by Monte Carlo and losses due to the limited mass range are taken into account. The first uncertainties in the branching fractions are statistical and the second systematic.

State (X)	Efficiency	Events	Branching fraction
$f_2(1270)$	13.0%	406±17	$(2.2 \pm 0.1 \pm 0.2) \times 10^{-4}$
$f_0(1500)$	15.0%	31±14	$(1.5 \pm 0.7_{-0.4}^{+0.9}) \times 10^{-5}$
$f_0(1710)$	15.2%	51±13	$(2.4 \pm 0.6_{-1.1}^{+0.8}) \times 10^{-5}$
$f_4(2050)$	15.4% ^a	61±20	$(2.8 \pm 0.9_{-0.6}^{+0.8}) \times 10^{-5}$
$f_0(2200)$	15.6%	99±22	$(4.6 \pm 1.0_{-0.9}^{+4.5}) \times 10^{-5}$

^aLinear interpolation between $f_0(1710)$ and $f_0(2200)$.

systematic uncertainty introduced by neglecting the σ .

VI. RESONANCES IN $\gamma K^+ K^-$

Fitting the $m_{K^+K^-}$ distribution between threshold and $3 \text{ GeV}/c^2$, the product branching fractions for $\psi(2S) \rightarrow \gamma X \rightarrow \gamma K^+ K^-$, where $X = f_2(1270)$, $f_2'(1525)$, and $f_0(1710)$, are obtained with a Pearson's χ^2/DOF of $37.4/39$ (Table II and Fig. 4). The high mass region is fitted with a three-body phase space background component and a combination of resonances: $f_4(2050)$, $f_0(2100)$, $f_2(2150)$, $f_0(2200)$, $f_2(2300)$, $f_2(2350)$, and $f_6(2510)$. The fit with $f_0(2200)$ and a phase space background is used to calculate the branching fractions in Table II (Fig. 4), and the other fits are used to estimate the systematic uncertainty. The $f_2(1270)$ branching fraction is a factor four larger than the BES1 measurement, but consistent with the measurement in $\gamma\pi^+\pi^-$ within the (large) uncertainties. The branching fraction into $f_0(1710)$ agrees with the BES1 measurement [4], and the $f_2'(1525)$ was part of the BES1 fit [4], but a branching fraction was never given. Removing the $f_2'(1525)$ here changed the log likelihood such that $R = 3.8$ (Eq. 3), which corresponds to a statistical significance of less than 2σ .

VII. UNCERTAINTIES

The statistical uncertainty includes the uncertainty in the number of events from data, continuum processes, and the small statistical uncertainty from the Monte Carlo simulation of $\psi(2S) \rightarrow \pi^+\pi^-\pi^0$, which is propagated into the uncertainty of the fitted branching fraction. Systematic uncertainties are inevitably introduced due to differences between simulation and reality; in this

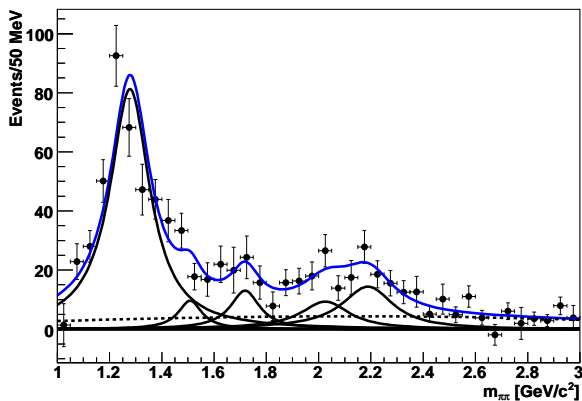


FIG. 3: Background reduced $m_{\pi^+\pi^-}$ distribution for $\gamma\pi^+\pi^-$ events (not efficiency corrected).

TABLE II: Number of selected events and product branching fractions in the $\psi(2S) \rightarrow \gamma X \rightarrow \gamma K^+ K^-$ channel. The efficiency at the central resonance mass is determined by Monte Carlo and losses due to the limited mass range are taken into account. The first uncertainties in the branching fractions are statistical and the second systematic.

State (X)	Efficiency	Events	Branching fraction
$f_2(1270)$	14.4%	39 ± 12	$(1.9 \pm 0.6^{+1.0}_{-0.6}) \times 10^{-5}$
$f_2'(1525)$	15.6%	15 ± 10	$(6.9 \pm 4.4^{+4.1}_{-2.1}) \times 10^{-6}$
$f_0(1710)$	16.3%	70 ± 14	$(3.1 \pm 0.6^{+1.1}_{-0.7}) \times 10^{-5}$

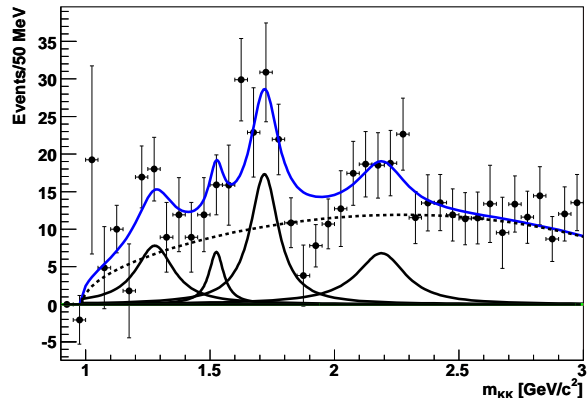


FIG. 4: Background reduced $m_{K^+K^-}$ distribution for $\gamma K^+ K^-$ events (not efficiency corrected).

case these are associated with MDC tracking, the kinematic fit, and particle identification (Table III). The detection efficiency for any state also depends on the angular distribution of the decay. For $J^{PC} = 2^{++}$ states, the angular distribution is determined up to two real parameters, x and y . In section VIII these are fitted to $\psi(2S) \rightarrow \gamma f_2(1270) \rightarrow \gamma\pi^+\pi^-$ data, and two different sign solutions are found. The overall detection efficiency of the two cases have a relative difference of 2.3% in $\gamma\pi^+\pi^-$ and 2.8% in $\gamma K^+ K^-$; this uncertainty is added quadratically into the overall systematic uncertainty for the $J^{PC} = 2^{++}$ and 4^{++} states.

TABLE III: Sources of systematic uncertainty to the branching fractions. Fit uncertainties are not included.

Source of uncertainty	
Number of $\psi(2S)$ [13]	4%
Charged tracks [3]	4%
Photon ID [26]	2%
Trigger [3]	<0.5%
Kinematic fit [27]	6%
Eff. variation with (x,y) $m_{\pi^+\pi^-}$	2.3%
Eff. variation with (x,y) $m_{K^+K^-}$	2.8%

The main source of systematic uncertainty is the choice of fit function, where the modeling of the background plays a major part. The $\psi(2S) \rightarrow \pi^+\pi^-\pi^0$ also contributes to the systematic uncertainty, since the branching fraction from the BESII measurement [12] has a relative uncertainty of 14.5%, which for $\psi(2S) \rightarrow \gamma\pi^+\pi^-$ corresponds to ~ 15 events in the region between 1 and 3 GeV/ c^2 . In the fit to $m_{\pi^+\pi^-}$, a few weak background sources are ignored; these add up to ~ 5 events in the region between 1 GeV/ $c^2 < m_{\pi\pi} < 2.5$ GeV/ c^2 . There could also be a contribution from unknown background and non-resonant production. The uncertainty introduced from these sources is investigated by adding a three-body phase space component to the fit, which converges to ~ 150 events between $m_{\pi\pi} = 1$ and 3 GeV/ c^2 . This is a component which is necessary to fit the data, $P_{\chi^2}(64, 1) < 0.0001$. The corresponding background component in $m_{K^+K^-}$ is more prominent (Fig. 4), and the branching fractions of some possible background sources are not yet measured. To investigate how the uncertainty in the background estimate influences the branching fractions in $\gamma\pi^+\pi^-$ and γK^+K^- , the best fit

is compared to a fit with a background fraction which is 50% smaller and 50% larger. The overall uncertainty introduced by the fit function is investigated by taking the minimum, and the maximum, value of the branching fraction for each specific resonance, with different resonance combinations and different size background components, and comparing this with the best fit. After adding the uncertainties in quadrature, we obtain the systematic errors in Tables I and II.

VIII. ANGULAR DISTRIBUTION OF $\psi(2S) \rightarrow \gamma f_2(1270) \rightarrow \gamma\pi^+\pi^-$

The radiative decay of a vector state [such as the J/ψ or $\psi(2S)$] into a tensor state [such as the light quark tensor $f_2(1270)$], which decays further into two pseudoscalars, has an angular distribution, which is determined by two real parameters: $x = A_1/A_0$ and $y = A_2/A_0$ [28, 29]. Here A_0 , A_1 , and A_2 are the helicity amplitudes for projection zero, one and two, respectively.

$$W(\theta_\gamma, \theta_M, \phi_M) = 3x^2 \sin^2 \theta_\gamma \sin^2 2\theta_M + (1 + \cos^2 \theta_\gamma) \left[(3 \cos^2 \theta_M - 1)^2 + \frac{3}{2} y^2 \sin^4 \theta_M \right] \quad (4)$$

$$+ \sqrt{3} x \sin 2\theta_\gamma \sin 2\theta_M \left[3 \cos^2 \theta_M - 1 - \frac{\sqrt{6}}{2} y \sin^2 \theta_M \right] \cos \phi_M + \sqrt{6} y \sin^2 \theta_\gamma \sin^2 \theta_M (3 \cos^2 \theta_M - 1) \cos 2\phi_M.$$

In the BESII cylindrical geometry, the z -axis is defined by the beam, θ_γ is the polar angle of the direct photon, and θ_M is the polar angle of one of the pions with respect to the γ -direction in the $f_2(1270)$ rest frame. The last parameter, ϕ_M , is the azimuthal angle of the same pion in the $f_2(1270)$ rest frame. By convention $\phi = 0$ lies in the plane defined by the electron beam and the photon in the $f_2(1270)$ rest frame. Predictions for x , y have been based on perturbative QCD [30], helicity two suppression [31], or, for instance, assumptions about the intermediate resonance being a glueball [32] (Table IV).

The W -distribution (Eq. 4) depends on the parameter x , but projections of the W -distribution onto the $\cos \theta_\gamma$ and the ϕ_M axes become independent of x , and the projection onto $\cos \theta_M$ is symmetric in x [19]. Therefore a three-dimensional analysis of many events is needed in order to determine the size and the sign of x [25, 29, 33]. The 172 events with $|m_{\pi^+\pi^-} - m_{f_2(1270)}| < 0.5\Gamma_{f_2(1270)}$ (mass and width from Ref. [1]) are fitted with a log likelihood fit. Continuum (15.4 events after scaling) and $\psi(2S) \rightarrow \pi^+\pi^-\pi^0$ (5.6 events after scaling) backgrounds are treated as scaled opposite sign contributions. The detection efficiency is determined using Monte Carlo modeling. Here, the cylindrical structure and the event selec-

TABLE IV: Helicities in different decay models and in measurement of $J/\psi \rightarrow \gamma f_2(1270) \rightarrow \gamma\pi^+\pi^-$. x and y are defined in the text.

Model	x	y
E1, low energy photon, pQCD [30]	$\sqrt{3}$	$\sqrt{6}$
Krammer, high energy photon [30]	0	0
Krammer at $\psi(2S) \rightarrow \gamma f_2(1270)$ [30]	0.68	0.45
Close [31]	$\sqrt{3}/2$	0
Ward glueball [32]	-0.85	-1.0
J/ψ BESII [22]	0.89 ± 0.02	0.46 ± 0.02
J/ψ Crystal Ball [29]	0.88 ± 0.13	0.04 ± 0.19
J/ψ MARK III [25]	0.96 ± 0.07	0.06 ± 0.08

tion requirements give a detection efficiency with dips at the end-caps in $\cos \theta_\gamma$ (as in MARKIII [25]). The detection efficiency is relatively isotropic in $\cos \theta_M$ but varies strongly with ϕ_M , where minima are obtained at $\phi_M = 0, \pi$, and 2π ; in these angular regions mesons can be close to the beam directions. Since both θ_γ and ϕ_M suffer from large acceptance correction effects, the θ_M distribution is the most powerful analyzer.

An angular fit to the three-dimensional $\psi(2S) \rightarrow \gamma f_2(1270) \rightarrow \gamma \pi^+ \pi^-$ distribution gives two solutions for x and y (Table V). The component with helicity two, y , is well determined whereas the component with helicity one, x , is essentially undetermined, mainly due to acceptance losses. The 1σ uncertainty in the fits is stated next to the fit result in Table V; these are equivalent to the statistical uncertainties from data and background.

Systematic uncertainties are listed in Table VI. The effects of insufficiently understood acceptance was investigated in Ref. [34] by comparing the fit to $\psi(2S) \rightarrow \gamma \chi_{c0}$ data with the known angular distribution, revealing a large systematic uncertainty in x . The effect of $\psi(2S) \rightarrow \gamma \pi^+ \pi^-$ background not resonating in $f_2(1270)$ is investigated by varying the invariant mass region, and effects of misidentified contributions within the data set are investigated by comparing the fit with and without continuum and $\psi(2S) \rightarrow \pi^+ \pi^- \pi^0$ contributions. Muon contamination is automatically part of the opposite sign continuum sample, and, since simulation showed no $\psi(2S) \rightarrow \mu^+ \mu^-$ contribution and less than a 1% $e^+ e^- \rightarrow \mu^+ \mu^-$ contribution within the region, these are assumed to be negligible. Misidentification of $\gamma K^+ K^-$ events is estimated to give a contribution of 0.6 events within the region and systematic uncertainties from the generator input-output are negligible. When the correlation between the uncertainties in x and y is unknown the maximum is assumed, *i.e.* 1 and -1 for the positive and the negative solution respectively, for nonresonant events and misidentified background. The overall correlation ρ between systematic uncertainties σ is calculated as

$$\rho = \sum_i \frac{\rho_i \sigma_{xi} \sigma_{yi}}{\sigma_x \sigma_y} \quad (5)$$

where i runs over all the systematic uncertainties [34].

IX. CONCLUSION AND DISCUSSION

The branching fraction of $\psi(2S) \rightarrow \gamma f_0(1710)$ is measured in both the $\pi^+ \pi^-$ and the $K^+ K^-$ decays. Both results are close to the one previous measurement from BES [4]. The ratio between $f_0(1710) \rightarrow \pi^+ \pi^-$ and $f_0(1710) \rightarrow K^+ K^-$ is found to be $(77 \pm 72)\%$, with a

TABLE V: The relative fraction of helicity one x and two y , to helicity zero in $\psi(2S) \rightarrow \gamma f_2(1270) \rightarrow \gamma \pi^+ \pi^-$. With the given number of events a preferred solution cannot be chosen. The first uncertainty is the 1σ -deviation in the fit, *i.e.* the statistical uncertainty, the second is systematic.

Positive solution	Negative solution
$x = 0.20 \pm 0.09 \pm 0.25$	$x = -0.26 \pm 0.09 \pm 0.24$
$y = -0.26 \pm 0.08 \pm 0.05$	$y = -0.25 \pm 0.09 \pm 0.06$
$\rho_{stat} = 0.53$	$\rho_{stat} = -0.43$
$\rho_{sys} = 0.44$	$\rho_{sys} = -0.41$

TABLE VI: Systematic uncertainties in the angular distribution fit.

Source of uncertainty	Positive			Negative		
	σ_x	σ_y	ρ	σ_x	σ_y	ρ
Angular acceptance	0.18	0.05	0.24	0.18	0.05	-0.24
Non-resonant events (Fit region variation)	0.14	0.02	1	0.12	0.03	-1
Misidentified background (With/without bg red.)	0.11	0.01	1	0.10	0.00	-1
Overall	0.25	0.05	0.44	0.24	0.06	-0.41

TABLE VII: The ratio $BR(\psi(2S) \rightarrow \gamma X)/BR(J/\psi \rightarrow \gamma X)$ for comparison with the 12 % Rule. The J/ψ branching fractions in the middle column are taken from [22, 23], and those in the right most column are taken from the Particle Data Group [1].

X	BES [22, 23]	PDG [1]
$f_2(1270) \rightarrow \pi^+ \pi^-$	$24 \pm 6\%$	$28 \pm 6\%$
$f_0(1500) \rightarrow \pi^+ \pi^-$	$22 \pm 27\%$	$> 5 \pm 4\%$
$f_0(1710) \rightarrow \pi^+ \pi^-$	$9 \pm 5\%$	$14 \pm 18\%$
$f_2(1270) \rightarrow K^+ K^-$	-	$60 \pm 45\%$
$f_2'(1525) \rightarrow K^+ K^-$	$4 \pm 6\%$	$3 \pm 4\%$
$f_0(1710) \rightarrow K^+ K^-$	$6 \pm 5\%$	$7 \pm 4\%$

large uncertainty mainly from the $K^+ K^-$ measurement. The potential glueball, the $f_0(1500)$, is accepted at the 5%-level in $\gamma \pi^+ \pi^-$. It has been seen in $J/\psi \rightarrow \gamma \pi^+ \pi^-$ [22], but this is a first measurement in $\psi(2S)$ radiative decays. The $f_2'(1525)$ is at the verge of being accepted at the 5%-level in $\gamma K^+ K^-$. The $f_2'(1525)$ has a strong signal in $J/\psi \rightarrow \gamma K^+ K^-$ [23] and was part of the fit in the BES I $\psi(2S) \rightarrow \gamma K^+ K^-$ analysis [4], but a branching fraction was never given. The region above 2 GeV/ c^2 has an enhancement both in $\pi^+ \pi^-$ and $K^+ K^-$. In $\pi^+ \pi^-$, the region is fitted with two resonances: the $f_4(2050)$ and the $f_0(2200)$. Both of these have been detected before in pseudoscalar final states in radiative J/ψ -decays [1]. In $K^+ K^-$, the same region has a rather uniform distribution with an enhancement around the $f_0(2200)$. The invariant mass distribution from $\psi(2S)$ decays is similar to the previously measured J/ψ case but due to the limited number of events here, a partial wave analysis is not feasible. One problem when comparing the J/ψ and the $\psi(2S)$ fit in $m_{\pi^+ \pi^-}$ is that in J/ψ there is destructive interference between the $f_0(2020)$ and the $f_0(1710)$ causing a dip at ~ 1.8 GeV/ c^2 . There is also destructive interference around 1.5 GeV/ c^2 , which shifts the peak of the $f_0(1500)$ to lower values than the pole position [22]. This pattern is not reproduced if we, as in this analysis, assume incoherence. The ratio $BR(\psi(2S) \rightarrow \gamma X)/BR(J/\psi \rightarrow \gamma X)$ is presented in Table VII for a few final states X for comparison with the

12%-rule.

Can we use the branching fractions to understand what goes on during the decay process? In an old prediction by Lipkin [35], different pQCD and pQED $\psi \rightarrow \gamma 2^{++}$ decay diagrams are compared under the assumption of isospin symmetry. The upper diagram in Fig. 5 gives the ratio

$$R = \frac{\Gamma(\psi(2S) \rightarrow \gamma f_2'(1525))}{\Gamma(\psi(2S) \rightarrow \gamma f_2(1270))} = 0.5 \quad (6)$$

and the lower gives $R \approx 8\%$. The analysis presented here gives a ratio of $\approx 4\%$ whereas corresponding measurement in J/ψ gave $R = 26\%$. From another pQCD diagram with photon radiation and subsequent hadron formation, Close predicted [31]

$$\frac{BR(\psi \rightarrow \gamma 0^+)}{BR(\psi \rightarrow \gamma 2^+)} = \frac{2}{7} \quad (7)$$

under the assumption of quark-antiquark pair formation with $L_z = 1$ and identical coupling between glue and scalar and glue and tensor. This can unfortunately not be compared to the present data since $BR(f_0(1710) \rightarrow K^+K^-)$ is unknown.

Acknowledgments

The BES collaboration thanks the staff of BEPC and computing center for their hard efforts. This work is supported in part by the National Natural Science Foundation of China under contracts Nos. 10491300, 10225524,

10225525, 10425523, the Chinese Academy of Sciences under contract No. KJ 95T-03, the 100 Talents Program of CAS under Contract Nos. U-11, U-24, U-25, and the Knowledge Innovation Project of CAS under Contract Nos. U-602, U-34 (IHEP), the National Science Foundation of China under Contract No. 10225522 (Tsinghua University), the Department of Energy under Contract

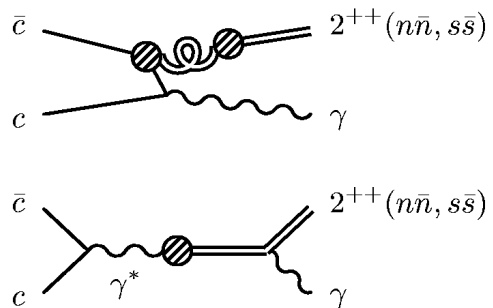


FIG. 5: Using perturbative QCD and QED, the process $\psi \rightarrow \gamma 2^{++}(q\bar{q})$ has an affinity for $s\bar{s}$ and $n\bar{n}$, which depends on the preferred diagram [35]. Lipkin predicted a ratio between $s\bar{s}$ and $n\bar{n}$ of 50% for the upper diagram and 8% for the lower, without taking phase space into account.

No. DE-FG02-04ER41291 (U. Hawaii), the Royal Physiographic Society in Lund Sweden, the Uppsala University Graduate School ΔU , the Sederholm Foundation, and the Gertrud Thelin foundation at Uppsala University.

-
- [1] W. M. Yao *et al.*, Journal of Physics G **33**, 1 (2006).
[2] N. Brambilla *et al.* (QWG and Topic conveners), *Heavy Quarkonium Physics* (CERN Yellow Reports, 2004).
[3] M. Ablikim *et al.* (BES collaboration), Phys. Rev. Lett. **99**, 011802 (2007).
[4] J. Z. Bai *et al.* (BES collaboration), Phys. Rev. D **67**, 032004 (2003).
[5] E. Eichten, K. Gottfried, T. Kinoshita, K. D. Lane, and T. M. Yan, Phys. Rev. D **17**, 3090 (1978).
[6] T. Appelquist, A. De Rújula, H. D. Politzer, and S. L. Glashow, Phys. Rev. Lett. **34**, 365 (1975).
[7] M. Chanowitz, Phys. Rev. D **12**, 918 (1975).
[8] L. Okun and M. Voloshin, ITEP-95-1976 (1976), (unpublished).
[9] S. J. Brodsky, T. A. DeGrand, R. R. Horgun, and D. G. Coyne, Phys. Lett. B **73**, 203 (1978).
[10] K. Koller and T. Walsh, Nucl. Phys. B **140**, 449 (1978).
[11] M. E. B. Franklin *et al.* (MARKII collaboration), Phys. Rev. Lett. **51**, 963 (1983).
[12] M. Ablikim *et al.* (BES collaboration), Phys. Lett. B **619**, 247 (2005).
[13] X. H. Mo *et al.*, High Energy Phys. and Nucl. Phys. **27**, 455 (2004), hep-ex/0407055.
[14] S. P. Chi, High Energy Phys. and Nucl. Phys. **28**, 1135 (2004), in Chinese.
[15] M. Ablikim *et al.* (BES collaboration), Phys. Rev. D **72**, 012002 (2005), hep-ex/0503040.
[16] J. Z. Bai *et al.* (BES collaboration), Nucl. Instr. and Meth. A **344**, 319 (1994).
[17] J. Z. Bai *et al.* (BES collaboration), Nucl. Instr. and Meth. A **458**, 627 (2001).
[18] M. Ablikim *et al.* (BES collaboration), Nucl. Instr. and Meth. A **552**, 344 (2005), physics/0503001.
[19] A. Lundborg, Ph. D. thesis, Uppsala University (2007), <http://publications.uu.theses/abstract.xsql?dbid=7460>.
[20] M. Ablikim *et al.* (BES collaboration), Phys. Lett. B **614**, 37 (2005), hep-ex/0407037.
[21] M. Ablikim *et al.* (BES collaboration), Phys. Rev. D **70**, 112007 (2004), hep-ex/0410031.
[22] M. Ablikim *et al.* (BES collaboration), Phys. Lett. B **642**, 441 (2006), hep-ex/0603048.
[23] J. Z. Bai *et al.* (BES collaboration), Phys. Rev. D **68**, 052003 (2003), hep-ex/0307058.
[24] B. S. Zou, Eur. Phys. J. A. **16**, 537 (2003).
[25] R. M. Baltrusaitis *et al.* (MARKIII collaboration), Phys. Rev. D **35**, 2077 (1987).
[26] J. Z. Bai *et al.* (BES collaboration), Phys. Rev. D **69**, 012003 (2004).

- [27] J. Z. Bai *et al.* (BES collaboration), Phys. Rev. D **69**, 072001 (2004).
- [28] P. K. Kabir and A. J. G. Hey, Phys. Rev. D **13**, 3161 (1976).
- [29] C. Edwards *et al.* (Crystal Ball collaboration), Phys. Rev. D **25**, 3065 (1982).
- [30] M. Krammer, Phys. Lett. B **74**, 361 (1978).
- [31] F. E. Close, Phys. Rev. D **27**, 311 (1983).
- [32] B. F. L. Ward, Phys. Rev. D **33**, 1900 (1986).
- [33] G. Alexander *et al.* (PLUTO collaboration), Phys. Lett. B **76**, 652 (1978).
- [34] M. Ablikim *et al.* (BES collaboration), Phys. Rev. D **70**, 092004 (2004).
- [35] H. J. Lipkin and H. R. Rubinstein, Phys. Lett, B **76**, 324 (1978).